Supporting Information

The Origin of High Na^+ Ion Conductivity in $Na_{1+x}Zr_2Si_xP_{3-x}O_{12}$ NASICON Materials

Judith Schütt,[a,b] Fiona Pescher,[b] Steffen Neitzel-Grieshammer[b,c]

[a.] Helmholtz-Institut Münster (IEK-12), Forschungszentrum Jülich GmbH, Corrensstraße 46, 48149 Münster, Germany.

[b.] Institute of Physical Chemistry, RWTH Aachen University, Landoltweg 2, 52056 Aachen, Germany.

[c.] JARA-HPC, RWTH Aachen University and Forschungszentrum Jülich GmbH, 52056 Aachen, Germany.

Table S1. Averaged bond distances $\bar{d}$ of Na1-O, Na2-O, Na3-O, P-O, Si-O, Zr-O in monoclinic NASICON structure of composition $Na_{1+x}Zr_2Si_xP_{3-x}O_{12}$ (x = 0 – 3).

	x = 0	x = 1	x = 2	x = 3
$\bar{d}$(Na1-O)[Å]	2.54 ± 0.06	2.56 ± 0.17	2.54 ± 0.16	2.49 ± 0.05
$\bar{d}$(Na2-O)[Å]	2.46 ± 0.13	2.51 ± 0.13	2.55 ± 0.17	2.60 ± 0.18
$\bar{d}$(Na3-O)[Å]	2.48 ± 0.16	2.51 ± 0.14	2.53 ± 0.10	2.56 ± 0.11
$\bar{d}$(P-O) [Å]	1.54 ± 0.04	1.54 ± 0.01	1.55 ± 0.01	
$\bar{d}$(Si-O) [Å]		1.63 ± 0.01	1.63 ± 0.01	1.64 ± 0.00
$\bar{d}$(Zr-O) [Å]	2.07 ± 0.03	2.08 ± 0.07	2.09 ± 0.07	2.08 ± 0.05

Table S2. Bond distances $\bar{d}$ of Na1-O, Na2-O, Na3-O, P-O, Si-O, Zr-O in monoclinic NASICON structure of composition $Na_3Zr_2Si_2PO_{12}$ (x = 1) determined experimentally[1,2] and by means of DFT[3] at RT.

	$x = 2^1$	$x = 2^2$	$x = 2^3$
$\bar{d}$(Na1-O)[Å]	2.61	2.70	2.53
$\bar{d}$(Na2-O)[Å]	2.70	2.59	2.58
$\bar{d}$(Na3-O)[Å]	2.72	2.55	2.53
$\bar{d}$(P-O) [Å]	1.54	1.59	1.55
$\bar{d}$(Si-O) [Å]	1.55	1.59	1.64
$\bar{d}$(Zr-O) [Å]	2.10	2.08	2.10

Table S3. Averaged bond distances $\bar{d}$ of Na1-O, Na2-O, Na3-O, P-O, Si-O, Zr-O in rhombohedral NASICON structure of composition $Na_{1+x}Zr_2Si_xP_{3-x}O_{12}$ (x = 0 – 3).

	x = 0	x = 1	x = 2	x = 3
$\bar{d}$(Na1-O)[Å]	2.54 ± 0.07	2.54 ± 0.17	2.54 ± 0.14	2.44
$\bar{d}$(Na2-O)[Å]	2.45 ± 0.12	2.49 ± 0.17	2.54 ± 0.16	2.57 ± 0.03
$\bar{d}$(P-O) [Å]	1.54 ± 0.05	1.54 ± 0.02	1.54 ± 0.01	
$\bar{d}$(Si-O) [Å]		1.63 ± 0.01	1.64 ± 0.01	1.64
$\bar{d}$(Zr-O) [Å]	2.08 ± 0.03	2.08 ± 0.08	2.09 ± 0.07	2.08 ± 0.05

Table S4. Bond distances $\bar{d}$ of Na1-O, Na2-O, Na3-O, P-O, Si-O, Zr-O in monoclinic NASICON structure of composition $Na_3Zr_2Si_2PO_{12}$ (x = 1) determined experimentally at RT.[2]

	x = 1
$\bar{d}$(Na1-O)[Å]	2.62
$\bar{d}$(Na2-O)[Å]	2.67
$\bar{d}$(P-O) [Å]	1.55
$\bar{d}$(Si-O) [Å]	1.55
$\bar{d}$(Zr-O) [Å]	2.07

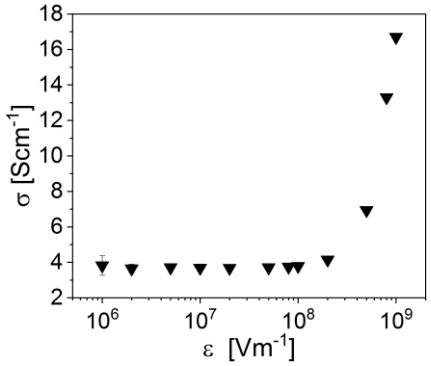

Figure S1. Conductivity σ in dependence of electric field strength ε in x-direction. In this study $\varepsilon = 10^7$ Vm^{-1} was applied.

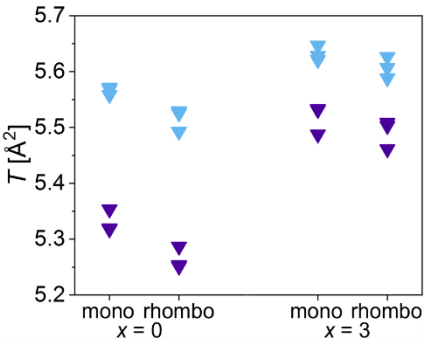

Figure S2. Area T of bottlenecks for sodium ion migration in initial/final state (purple) and transition state (blue) of rhombohedral and monoclinic structure with composition $x = 0$ and $x = 3$

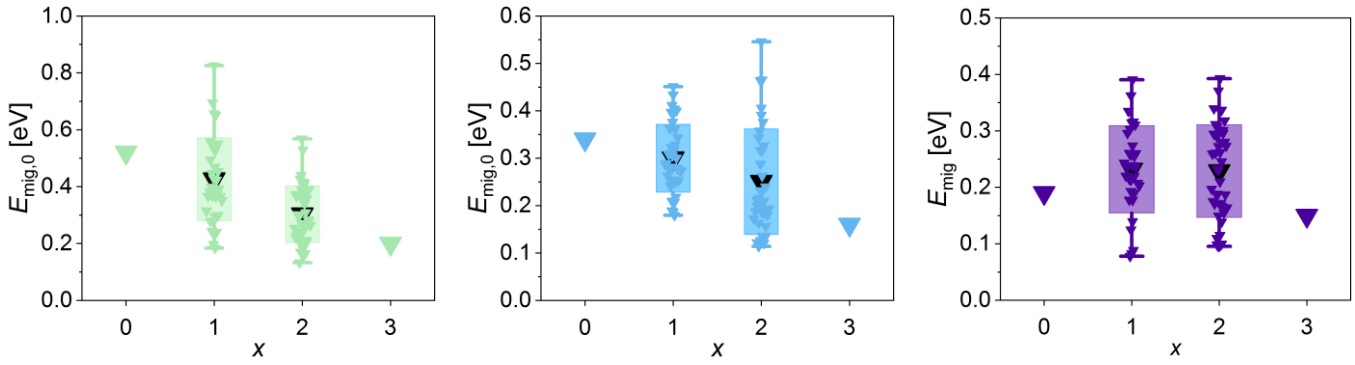

(a) Migration energies of 80° path. (b) Migration energies of 90° path. (c) Migration energies of 180° path.

Figure S3. Migration energies $E_{mig,0}$ in dependence of doping fraction x for 80° (a), 90° (b) and 180° (c) pathways in rhombohedral structure. All calculated migration energies (triangle), averaged migration energies (black triangles), standard deviations (box) and range between minimum and maximum values are shown.

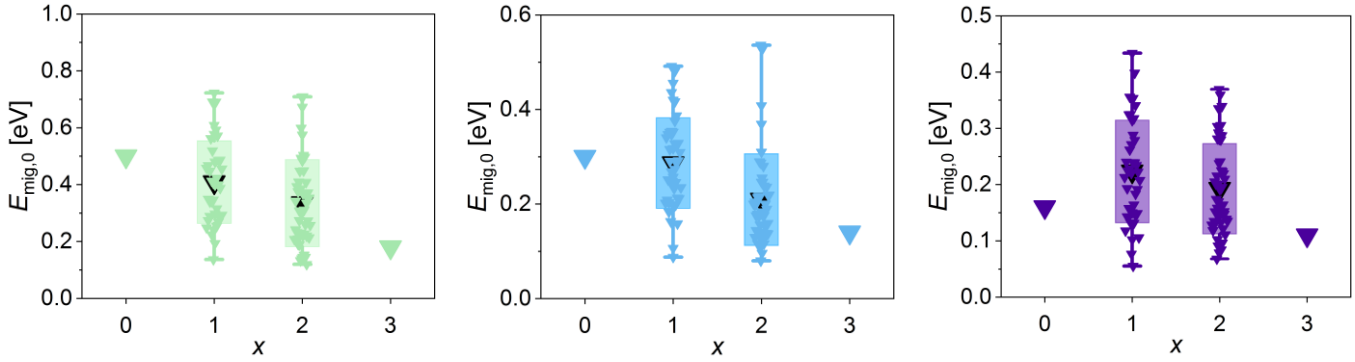

(a) Migration energies of 80° path. (b) Migration energies of 90° path. (c) Migration energies of 180° path.

Figure S4. Migration energies $E_{mig,0}$ in dependence of doping fraction x for 80° (a), 90° (b) and 180° (c) pathways in monoclinic structure. All calculated migration energies (triangle), averaged migration energies (black triangles), standard deviations (box) and range between minimum and maximum values are shown.

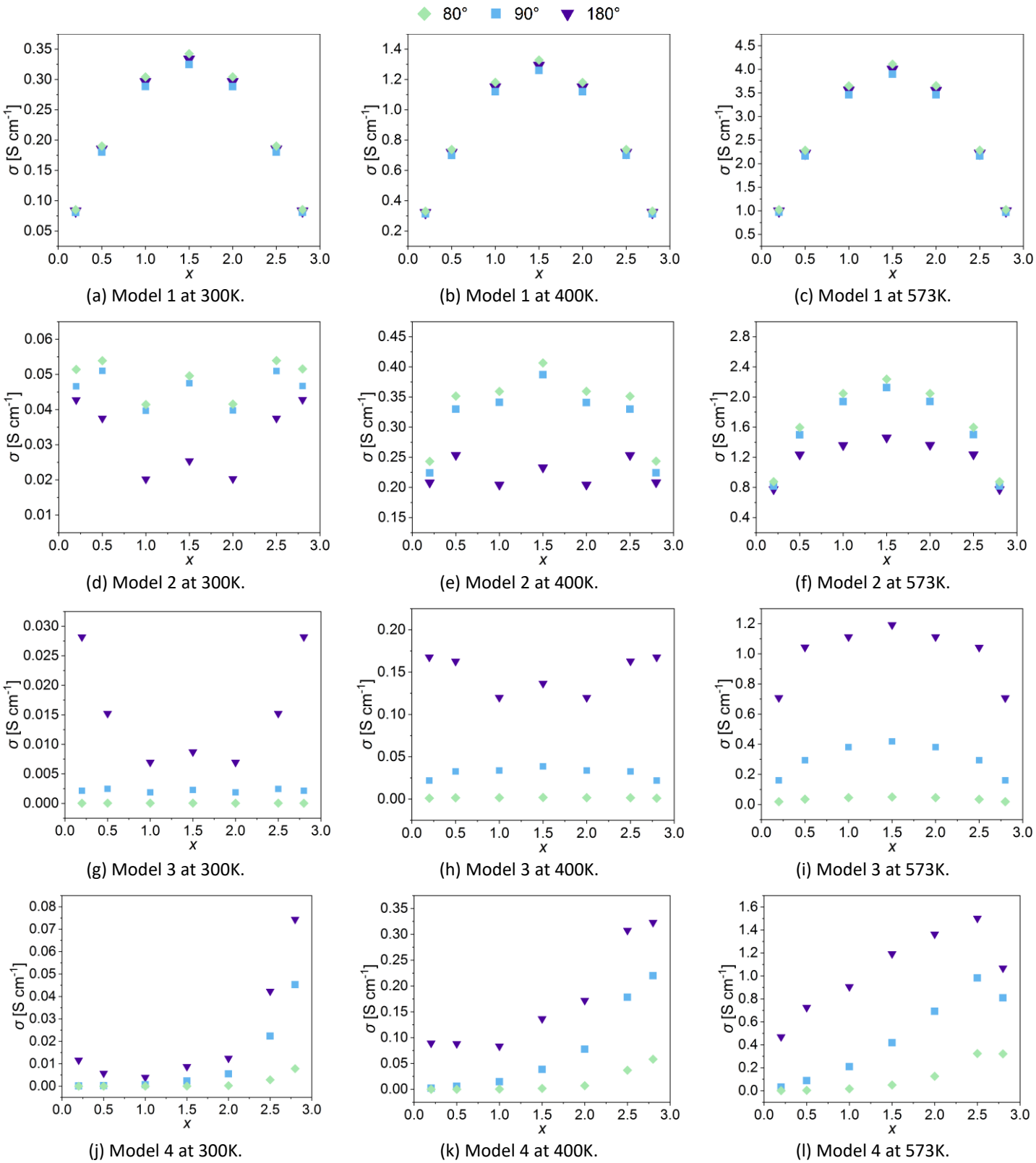

(a) Model 1 at 300K. (b) Model 1 at 400K. (c) Model 1 at 573K.

(d) Model 2 at 300K. (e) Model 2 at 400K. (f) Model 2 at 573K.

(g) Model 3 at 300K. (h) Model 3 at 400K. (i) Model 3 at 573K.

(j) Model 4 at 300K. (k) Model 4 at 400K. (l) Model 4 at 573K.

Figure S5. Partial conductivity resulting from 80° (green), 90° (blue) and 180° (purple) migration in rhombohedral $Na_{1+x}Zr_2Si_xP_{3-x}O_{12}$ (x = 0.2 – 2.8) at T = 300K, 400K, 573 K obtained from simulation using model 2 – 4.

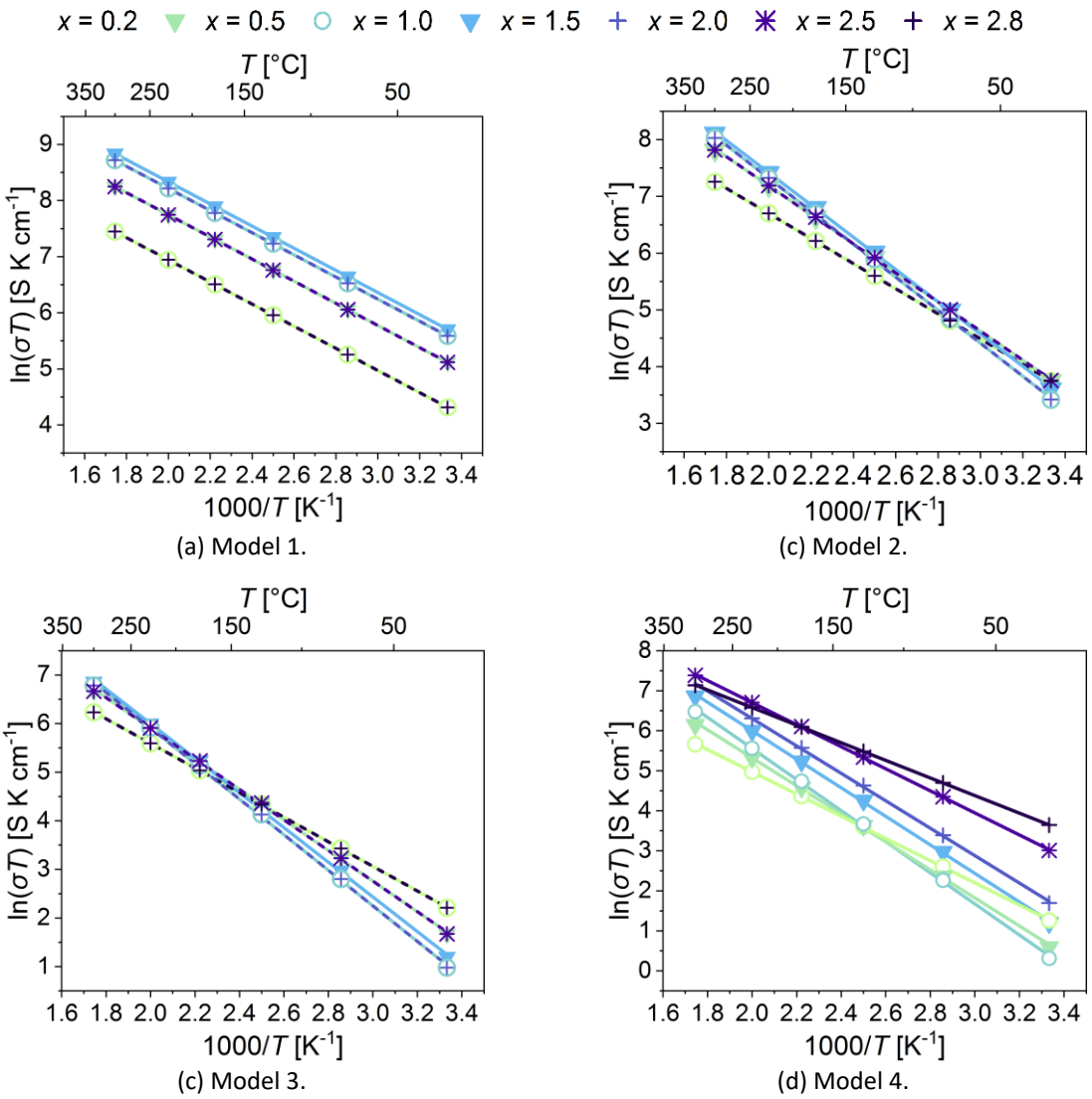

Figure S6. Arrhenius plots obtained from conductivities of simulations using model 1 – 4 of rhombohedral $Na_{1+x}Zr_2Si_xP_{3-x}O_{12}$ (x = 0.2 – 2.8) in the temperature range of T = 350 – 573 K in 10 × 10 × 10 cell.

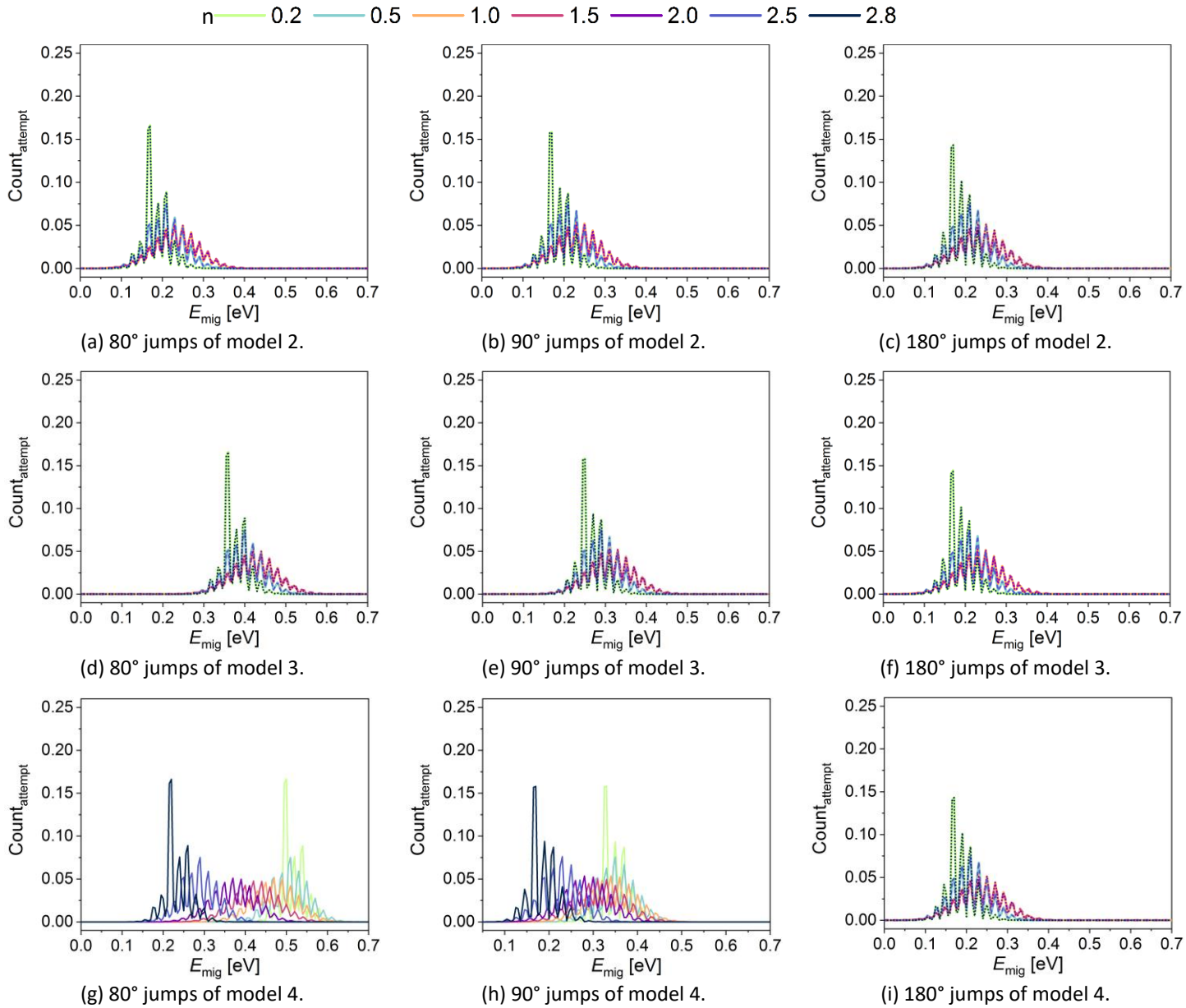

(a) 80° jumps of model 2. (b) 90° jumps of model 2. (c) 180° jumps of model 2.

(d) 80° jumps of model 3. (e) 90° jumps of model 3. (f) 180° jumps of model 3.

(g) 80° jumps of model 4. (h) 90° jumps of model 4. (i) 180° jumps of model 4.

Figure S7. Normalized energy-dependent number of attempted jumps in 80°, 90° and 180° direction in $Na_{1+x}Zr_2Si_xP_{3-x}O_{12}$ (x = 0.2 – 2.8) at T = 573 K of simulation using model 2 – 4.

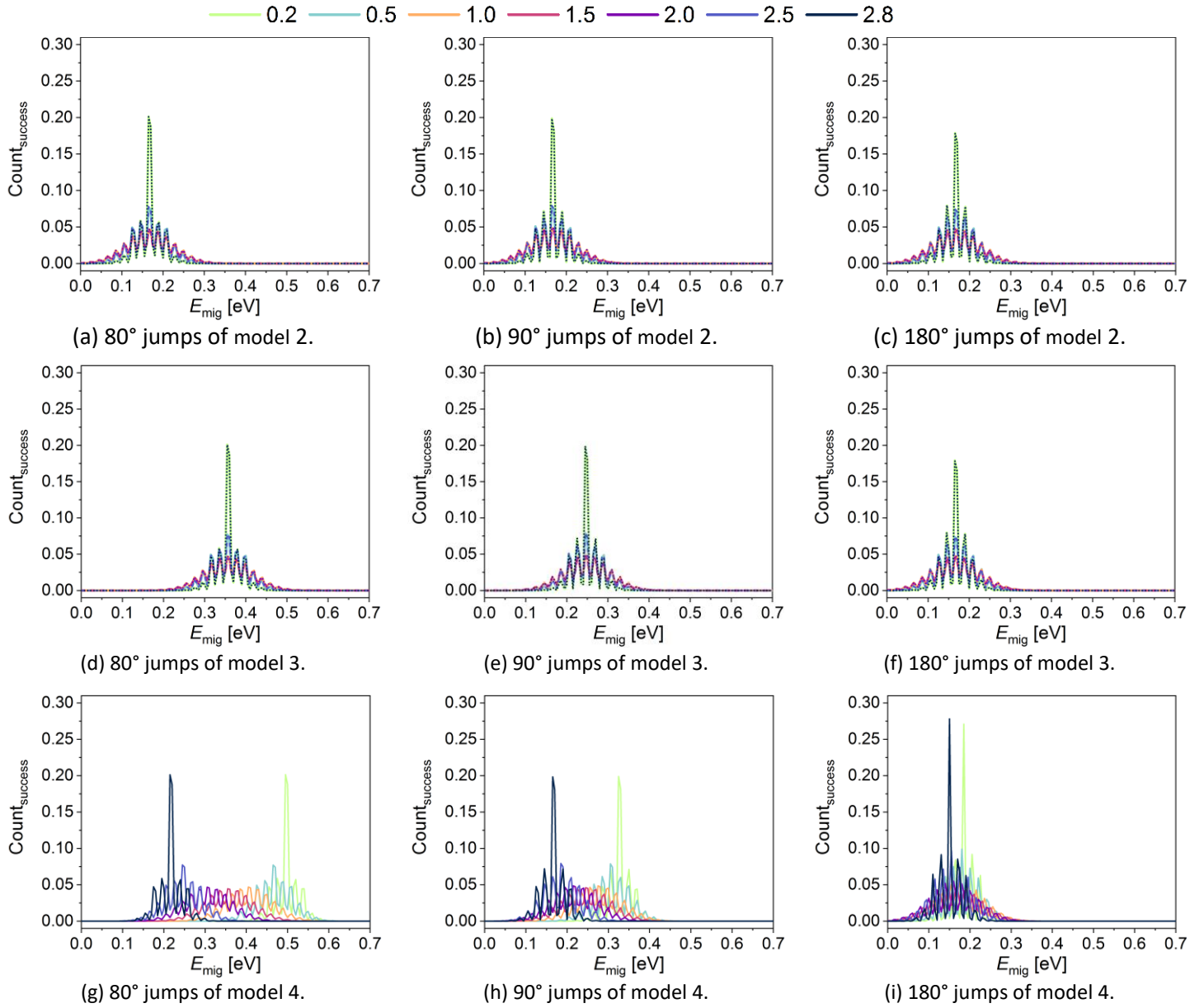

Figure S8. Normalized energy-dependent number of succeeded jumps in 80°, 90° and 180° direction in $Na_{1+x}Zr_2Si_xP_{3-x}O_{12}$ (x = 0.2 – 2.8) at T = 573 K of simulation of simulation using model 2 – 4.

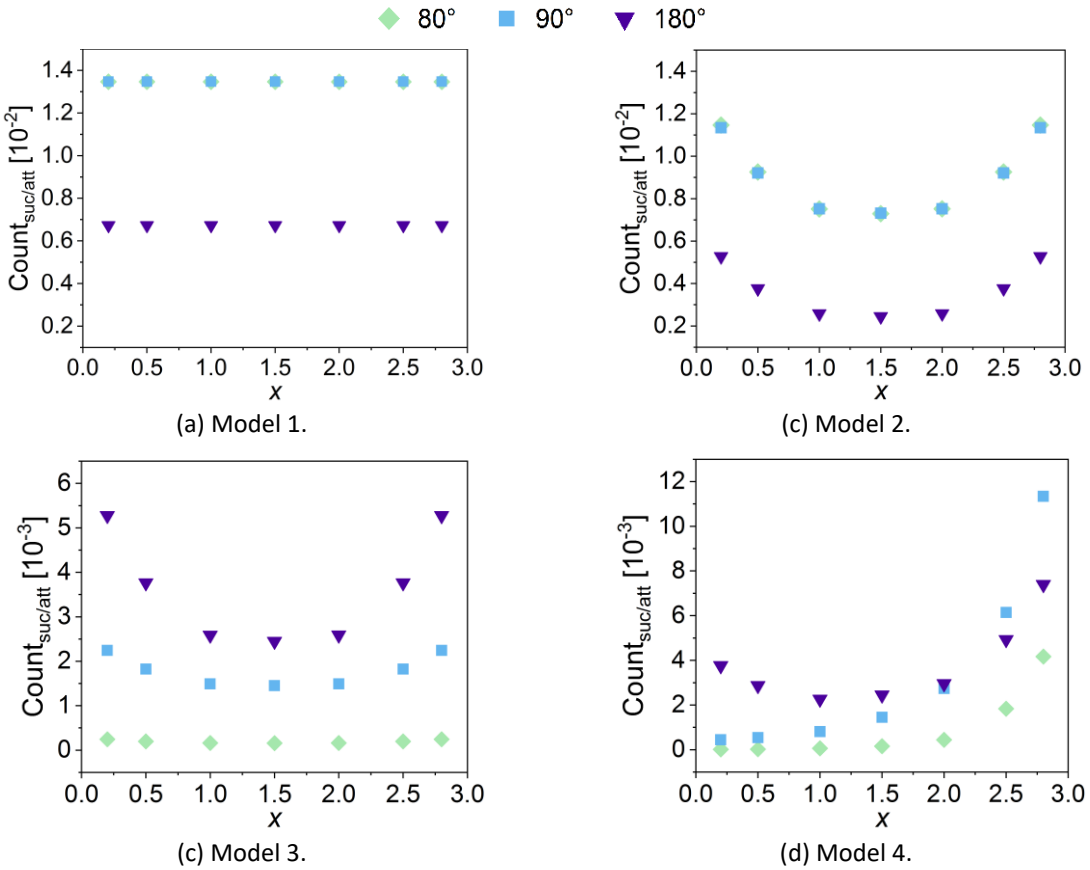

Figure S9. Ratio of succeeded to attempted jumps in 80° (green), 90° (blue) and 180° (purple) direction in $Na_{1+x}Zr_2Si_xP_{3-x}O_{12}$ (x = 0.2 — 2.8) at T = 573 K of simulation using model 2 – 4.

References

1 H.-P. Hong, Crystal structures and crystal chemistry in the system $Na_{1+x}Zr_2Si_xP_{3-x}O_{12}$, *Mater. Res. Bull.*, 1976, **11**, 173–182.

2 W. H. Baur, Dygas, JR, D. H. Whitmore and J. Faber, Neutron powder diffraction study and ionic conductivity of $Na_2Zr_2SiP_2O_{12}$ and $Na_3Zr_2Si_2PO_{12}$, *Solid State Ion.*, 1986, **18**, 935–943.

3 K. M. Bui, A. van Dinh, S. Okada and T. Ohno, Na-ion diffusion in a NASICON-type solid electrolyte: a density functional study, *Phys. Chem. Chem. Phys.*, 2016, **18**, 27226–27231.